

Research Paper

Structural Investigation and Photocatalytic Application of Sol-Gel Auto-Combustion Derived $ZnAl_2O_4$ Spinel for the Degradation of Organic Dye Pollutant

Muhammad Javed* and Naeem Akbar

Department of Physics, University of Kotli Azad Jammu and Kashmir, Kotli, 11100, Pakistan

*Corresponding author's email: javedbinyousuf@gmail.com

ARTICLE INFO

Article history:

Received: 15-02-2023

Revised: 21-11-2023

Accepted: 23-11-2023

Available online: 25-11-2023

Keywords:

Spinel,

Combustion,

photodegradation, Pollutant,

Crystal Violet

Abstract

In this study, we synthesized $ZnAl_2O_4$ aluminate via the sol-gel auto-combustion method and sintered it at 900°C . Rietveld refinement analysis of XRD data confirmed the formation of the normal spinel structure with the $Fd3m$ space group. The "crystallite size" was calculated by using the Debye-Scherrer and W-H plots and was found to be 78 and 91 nm, respectively. Field emission scanning electron microscopy (FESEM) investigation revealed the mixed morphology of synthesized aluminates with considerable porosity. The optical properties were "investigated" by using a UV-Vis spectrometer and the band gap was approximated to be 3.4 eV. The synthesized aluminate was also employed for the degradation of Crystal violet (CV) organic dye pollutants under solar light irradiation. It has been observed that the percentage degradation of dye was increased with contact time and significant removal of 80 % was achieved after 120 minutes. The degradation process followed the pseudo-first-order kinetic model. These insights might be significantly advantageous for environmental applications, including dye removal from aqueous solutions for wastewater remediation.

Introduction

Spinel metal oxides are a kind of ternary oxide having the chemical formula AB_2O_4 , where $A=Mg, Zn, Cu, Mn, Fe, Ba$, and $B=Mn, Cr, Al, Ni, Fe, Co$, etc. Tetrahedral interstices (A-site) are typically smaller in size than octahedral interstices (B-site). As a result, smaller cations prefer to have the A sites, whereas superior cations want to have the B sites (Bitla et al., 2015). Efforts are being made to "replace the conventional noble metal catalysts with oxide catalysts, which are equally economical and efficient. The oxide catalysts have noteworthy characteristics such as toxin resistance, a broad spectrum of adsorption, and reaction characteristics due to varying oxidation states, variable lattice spacing, and acidic or basic properties (Védrine, 2017). Investigations on numerous mixed oxides and supported systems indicated that the performance of these catalysts is governed by a new phase at the metal oxides interface, such as spinel or perovskite. As a result, the study of the catalytic activity of these pure spinel phases sparked a lot of interest. Spinel oxides are often found to be more suitable than their binary oxide counterparts due to their stability under the rigorous conditions that exist in industrial applications. Spinel oxides are extremely flexible regarding metal ions with various valences because of their stability. Spinel oxide possesses intriguing magnetic, electrical, and surface characteristics that affect how it is employed as a catalyst in a variety of applications, including oxidation of isobutene (Kirankumar & Sumathi, 2020), ethylene polymerization (El-Shobaky et al., 1999), oxidative dehydrogenation of H_2S (Grzybowska et al., 1998), ethane oxidation (Weckhuysen & Schoonheydt, 1999), oxidation of carbon monoxide." (Sickafus et al., 1999), etc.

Water-related issues are expected to deteriorate in the next decades, even in regions that are generally regarded to be water-rich. Attention to these challenges demands a large volume of research to identify effective new approaches for cleaning water at a lower cost with less energy, fewer chemicals, and less impact on nature (Robinson, 2008). For wastewater treatment, advanced oxidation processes (AOPs) such as photocatalysis, photo-Fenton, sonolysis, and sonophotocatalytic processes have been documented. Among all, photocatalytic oxidation triggered by narrow bandgap nanoparticles has drawn a lot of attention in recent years for treating contaminated water (which contains hazardous organic compounds and metal ions) (Lee et al., 2016). Various spinel-based semiconductor metal oxides such as $ZnGa_2O_4$, $ZnFe_2O_4$, $CuAl_2O_4$, and $CaBi_2O_4$, $BaCr_2O_4$ are used as photocatalysts (Boppana et al., 2010; Lv et al., 2009; Tang et al., 2004; D. Wang et al., 2003; Zhu et al., 2010). $ZnAl_2O_4$, among them, is a ternary oxide with a spinel structure that has drawn substantial interest as an advanced material in recent years due to its desirable properties low surface acidity, wide band gap, and excellent optical properties with various applications (Ianoş et al., 2014; Lee et al., 2016; Tian et al., 2009). As a result, it is being employed as a high-temperature material, sensors, electronic and optical materials, and catalysts (Anand et al., 2015; Ianoş et al., 2014; Motlounq et al., 2015; S.-F. Wang et al., 2015; Zhang et al., 2016). $ZnAl_2O_4$ with significant surface area and porous structure are crucial for catalytic processes. In general, numerous wet chemical routes have been employed for the

synthesis of zinc aluminate spinel-oxide which includes hydrothermal (Galetti et al., 2010), microwave combustion (Ballarini et al., 2009), co-precipitation (Tao et al., 2007), sol-gel method (Manikandan et al., 2014) and sol-gel auto-combustion method (Petcharoen & Sirivat, 2012). Among various wet chemical methods, the sol-gel auto-combustion route is a simple, fast, and energy-efficient route for the synthesis of metal oxide-based materials yielding high purity and chemically homogeneous powder (Akpan & Hameed, 2010; Sutka & Mezinskis, 2012). Appropriate selection of metal precursors and fuels like citric acid controls the combustion process and produces a fast and exothermic chemical reaction to form the compound (Anand & Kennedy, 2013). The synthesis route greatly influences the properties and applications of the materials. In this context, the aim of this study is to focus on the synthesis route, which greatly influenced the photocatalytic response of photocatalyst for the environmental pollutants by employing these spinel oxides and encounter the future challenges for improving the photocatalytic activity of metal oxide.

Experimental

Synthesis

The spinel ZnAl_2O_4 aluminate was synthesized by the wet chemical sol-gel auto-combustion method. Zinc nitrate and aluminium nitrate were used as precursors. The metal nitrates were used as oxidizers and citric acid as fuel for combustion. First zinc nitrate and aluminium nitrate were dissolved in DI water under constant stirring to form a transparent and homogeneous solution. The solution of citric was prepared in such that the nitrate to citrate ratio was 1:1. The aqueous nitrate solution was dropped into nitrate solution under continuous stirring and neutralization of the solution was obtained by adding ammonium hydroxide. The resulting solution was evaporated on a hot plate at 120° under stirring for about 4 hours, which resulted in a highly viscous gel. In order to expel a significant amount of gases from the gel, it was heated to a temperature of around 300°C . After a short heating time, the initiation temperature was attained, and the self-combustion process began. The resulting grey, fluffy, and pliable powder was collected, pulverized, and calcined in a muffle furnace for 10 hours at 900°C with a ramping rate of 5°C per minute. The choice of calcination temperature, such as 900°C in the case of ZnAl_2O_4 , in materials science and chemistry is typically based on several factors, including the desired properties of the final product and the specific synthesis method being employed. Here are some factors that may influence the selection of a calcination temperature for ZnAl_2O_4 : Phase Formation: The calcination temperature should be high enough to ensure the formation of the desired phase, in this case, ZnAl_2O_4 . Different materials have different temperature ranges at which they form specific phases. Researchers often consult phase diagrams and previous studies to determine the appropriate temperature range for phase formation. Kinetics of Reaction: Temperature has an effect on the rate of the reaction. Higher temperatures enhance more rapid kinetics in general. Frequently high temperatures, on the other hand, might cause sintering or other undesirable processes, therefore a balance must be established to reach the required phase without generating undesirable side reactions. Purity and crystallinity: The calcination temperature can impact the purity

and crystallinity of the final product. Higher temperatures might result in more complete crystallization and higher purity. Temperature is frequently optimized by researchers to attain a suitable level of crystallinity while minimizing impurities.

Fuels are compounds that may perform chemical interactions with oxygen to produce energy in the form of heat and light during combustion processes. To release energy, these processes often entail the breakdown of chemical bonds in the fuel molecules. As an organic acid, citric acid is more typically used in chemical reactions such as fermentation or as a reactant in some industrial processes than as a source of energy through combustion.

Photocatalytic activity measurement

The photocatalytic activity of ZnAl_2O_4 spinel oxide was investigated for the degradation of Crystal violet under UV-light irradiation. In the typical photocatalytic degradation experiment 50 ml of 10 ppm solution crystal violet (CV) solution, 0.1 g of ZnAl_2O_4 catalyst was added to a 100 ml beaker and placed in a dark condition for one hour with stirring to attain equilibrium adsorption. After that, the comprising solution was placed under sunlight. The aliquots were collected at regular intervals of time and absorbance for each interval was investigated by UV-Vis spectrometer over the experimental range of 400-750 nm.

Characterization

The synthesized sample was characterized by the X-rays diffraction (XRD) technique by the Regaku model. The XRD spectrum was scanned at room temperature in the two-theta range from 20° - 80° with a Cu-K λ radiation source. Further, various structural parameters have been investigated by using full prof software with the least square method. The morphology of the prepared sample was investigated by employing field emission scanning electron microscopy (FESEM Zeiss Merlin). The optical absorption study of CV dye was examined using UV-Vis spectroscopy (Date stream CE 3000 series spectrometer) with different intervals of time.

Results and Discussion

Structural Analysis

Figure 1(a) shows the room temperature XRD profile of ZnAl_2O_4 spinel in the two-theta range 20° - 80° . The diffractogram indicates a crystalline phase with the Bragg reflections peaks indexed and matched well with the joint committee on powder diffraction standards (JCPDS) published database with file number 05-0669 for ZnAl_2O_4 normal spinel (Sunder & Kumar, n.d.). The diffraction characteristics peaks corresponding to (220), (311), (400), (331), (422), (333), (440), (620), and (533) reflection of cubic spinel structure of ZnAl_2O_4 . Some impurities peaks were also observed in the XRD pattern indicates by the green star in Figure 1(a) which may arise at high calcination temperatures. Thermal decomposition: At high temperatures, some materials may thermally break down, leading to the synthesis of new compounds or the release of volatile species. These breakdown products may

disrupt the XRD pattern and appear as impurities. Sintering: When heated to high temperatures,

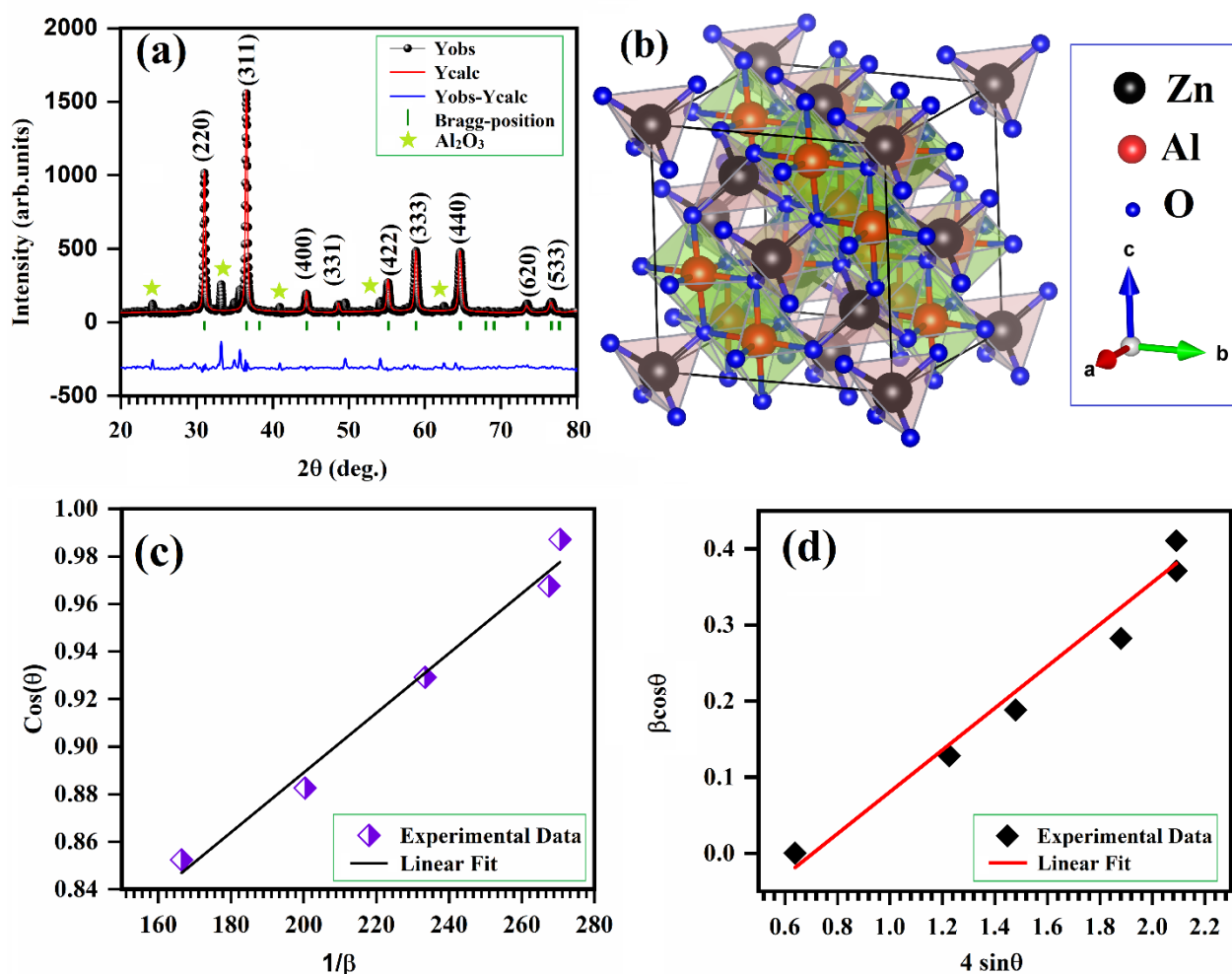


Figure 1. (a) Rietveld refined XRD profile of ZnAl_2O_4 (b) (D-S) plot (c) (W-H) Plot.

particles in the sample might sinter or fuse together, modifying the sample's microstructure and potentially distorting the diffraction pattern. The estimated crystallite size was uniform throughout the sample and was estimated by two theoretical methods and was elevated to be 78 and 91 nm respectively. Twinning in crystals, where two or more regions of a crystal have different orientations, can lead to additional diffraction peaks. These impurity peaks matched well with the JCPDS card number -046-01212 and are identified to come from the presence of the Al_2O_3 phase (Fakeeha et al., 2018). For further investigation of various structural parameters, the Rietveld refinement of XRD experimental data was performed by the Full Prof program and is shown in Figure 1(a). In the XRD refined pattern black ball indicates experimental data, the red line symbol represents the XRD diffraction pattern, the green vertical bar ticks show the position of Bragg reflections for the prepared zinc aluminate sample and the green star marks the impurity phase. The resulting parameters deduced from Rietveld refinement are highlighted in Table 1. Further, the average crystallite size is estimated by the Debye-Sherrer (D-S) equation and further compared with the size, deduced from the

Table 1. Structural results approximated from the Rietveld XRD profile analysis of ZnAl₂O₄ aluminate structure.

Aluminate System			ZnAl ₂ O ₄			
Structural Parameters	Space group	Fd $\bar{3}$ m	Atom	Wyckoff Positions		
	Lattice Parameters			x/a	y/b	Z/c
	$\alpha = \beta = \gamma$	90	Zn	0.12500	0.12500	0.12500
	a (Å)	8.1555	Al	0.12500	0.12500	0.12500
	b (Å)	8.1555	O	0.26360	0.26360	0.26360
	Unit Cell Volume (Å ³)	542.4401	Average Crystallite Size and Micro-strain			
Formula Sum	ZnAl ₂ O ₄		D _{D-S}	D _{W-H}	ϵ	
			78	91	2.7525×10^{-6}	
Reliable Factors	R _F (%)	R _B (%)	R _{exp} (%)	R _{wp} (%)	χ^2 (%)	
	13.9011	13.0014	9.8400	29.4000	1.8620	

Williamson -Hall (W-H). The former is expressed by the following expression (Selvanayaki et al., 2022):

$$D = k\lambda/\beta\cos\theta \quad (1)$$

Here, D represents the crystallite, k indicates the particle shape factor with a value of 0.9, λ is the CuK α source (0.154 nm) and θ is half of the Bragg reflections angle. The average crystallite size was found to be 78 nm as depicted in Figure 1(b). Further, the Crystallite size and strain were estimated by the W-H relation and can be expressed as (Mote et al., 2012):

$$\beta\cos\theta = kD/D + 4\epsilon\sin\theta \quad (2)$$

Where ϵ refers to the micro-strain induced in the lattice and other parameters have the usual meaning. The crystallite size and micro-strain were recorded as 91 nm and 2.7525×10^{-6} units respectively, as shown in Figure 1(c). The discrepancy in crystallite size values between the D-S and W-H plots was due to the integration of crystallite lattice strain in the W-H approach, which was caused by defects such as twinning, dislocation, distortion, and imperfection.

Microstructural Analysis

The surface morphology of sol-gel auto-combustion derived ZnAl₂O₄ spinel was observed by field emission scanning electron microscopy (FESEM). The FESEM images of zinc aluminate with low and high magnification are shown in Figure 2(a, c). The micrographs show that the synthesized sample exhibits a mixed morphology with loosely agglomerated grains having a porous-like nature which may be attributed to the release of volatile gases such as O₂, N₂, and CO₂ during the combustion process. Furthermore, the average size was recorded by considering certain selections from the FESEM micrograph by using image j software. The Gaussian fit gives the most probable average grain size and it has been estimated to be about 180 ± 5.80 nm as shown in Figure 2(b). The significance of porosity observed in FESEM images assists the photocatalysis depending on the following factors

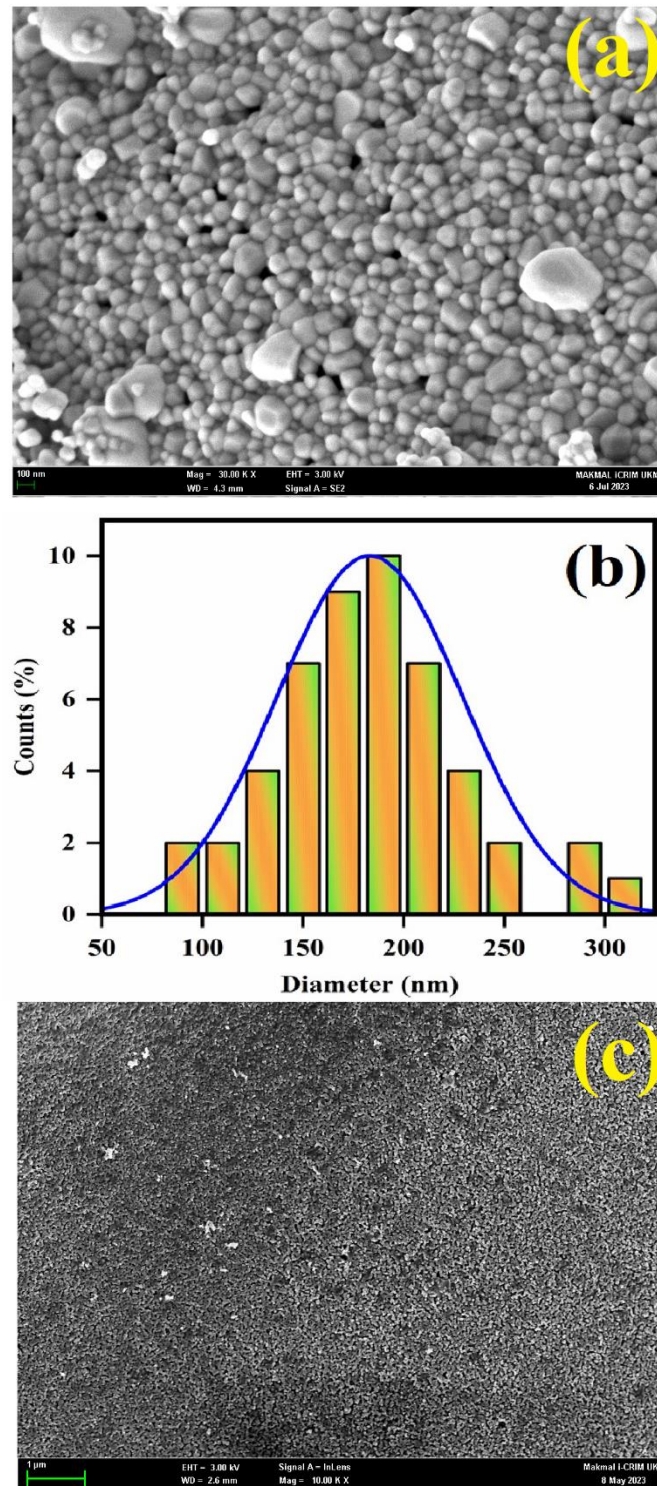


Figure 2. FESEM micrographs of (a, c) ZnAl_2O_4 aluminate with low and high magnification respectively, (b) particle size distribution for zinc aluminate.

Surface area: is the key parameter for photocatalysis a higher surface area can provide more active sites for photocatalytic reactions to occur. This can enhance the photocatalytic efficiency of the material by increasing the number of sites available for interactions with reactants. Adsorption: Since

porous materials offer a larger surface area, they may adsorb more reactants and contaminants onto their surfaces. This can be advantageous to photocatalysis because it facilitates more effective interaction between the reactants and the photocatalyst, boosting pollutant destruction. Transport of Species: Porosity may assist in the diffusion and transfer of reactants and products inside a material. This might help in the efficient use of the photocatalyst and lead to more rapid response rates. The optical characteristics of porous aluminates can differ from those of non-porous materials. Porous materials may trap and scatter light, which can increase light absorption and photocatalytic activity, particularly in the visible light spectrum.

Optical study

Figure 3(a) shows the room temperature UV-Vis spectra of zinc aluminate. Almost 378 nm indicated the band edge for the $ZnAl_2O_4$ catalyst. The band gap energy of the $ZnAl_2O_4$ nanocrystal was estimated by using the Tauc's equation (Srinatha et al., 2022):

$$(\alpha h\nu)^{1/n} = A(h\nu - E_g) \quad (3)$$

Where A is constant and varies with transition, $h\nu$ is photon energy input, E_g is the energy gap, α is the absorption coefficient, and h is the Planck constant.

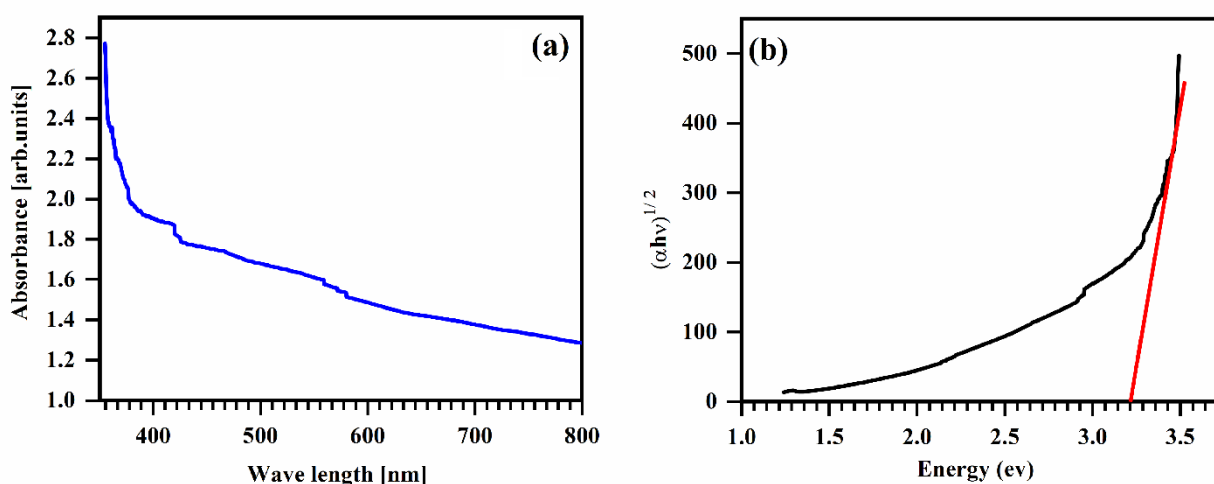


Figure 3. (a) Room temperature UV spectra of $ZnAl_2O_4$ photocatalyst (b) Tauc's plot

The value of the exponent n indicates whether the electronic transition is allowed or forbidden and whether it is direct or indirect. $n = 1/2$ for permissible and direct transitions, and $n = 3/2$ for forbidden and direct transitions. Also, $n = 2$ for allowed and indirect transitions, and $n = 3$ for forbidden and indirect transitions. In general, the permissible transitions lead to fundamental absorption processes, allowing $n = 1/2$ for direct and $n = 2$ for indirect transitions (Coulter & Birnie III, 2018). The value of n was chosen to be $1/2$ since $ZnAl_2O_4$ has a direct energy bandgap. By extrapolating the linear portion of the $(\alpha h\nu)^2$ vs. $h\nu$ plot to intercept on the horizontal energy axis as shown in Figure 3(b). The band

gap energy of ZnAl_2O_4 was to be 3.4 eV. A photocatalyst's band gap is a significant characteristic because it contributes to the range of light wavelengths (or energy) that the material can absorb and employ for photocatalytic processes. Here's how the 3.4 eV band gap compares to various spinel-based semiconductor metal oxides and typical photocatalysts: The band gap of TiO_2 varies between 3.0 and 3.2 eV depending on its phase (anatase, rutile, or brookite). It is one of the most recognized and most commonly utilized photocatalysts. The band gaps of spinel-type oxides can vary depending on the components involved and the crystal structure. A band gap of 3.4 eV is within a suitable range for semiconductor metal oxides utilized in photocatalysis.

Photocatalytic Analysis

Photocatalytic degradation

Figure 4(a) depicts the room temperature UV spectra for the degradation of Crystal violet (CV) dye using the synthesized ZnAl_2O_4 photocatalyst under the irradiation of sunlight. UV-visible spectra of CV show a strong adsorption band at 554 nm. No the photocatalytic activity of the ZnAl_2O_4 catalyst was tested under different UV-light intensities or at different solution pH values which might be due to the reason. The researchers may have had specific research objectives that did not include studying the catalyst's response to different UV-light intensities or pH values. Our focus might have been on other aspects of the catalyst's performance. After the addition of the photocatalyst, the adsorption spectra show a decreasing pattern with irradiation time representing the degradation of organic dye pollutants. Figure 4(b) shows the degradation efficacy of CV with time, from the degradation profile it has been observed that 80 % of dye degrades photochemical after 120 minutes. In the realm of photocatalysis, it is usual practice to compare the photocatalytic activity of one catalyst, such as ZnAl_2O_4 , to that of other photocatalysts. Comparative studies are frequently carried out by researchers to assess the effectiveness, stability, and performance of a novel catalyst in comparison to those of others. This helps in comprehending the catalyst's potential for use in a variety of processes, such as the formation of hydrogen or the purification of air. The significant removal of 80% of a dye like CV (Crystal Violet) after 120 minutes of degradation can be influenced by several factors. Photocatalyst type and activity: The photocatalyst utilized is significant. If a high activity photocatalyst, such as titanium dioxide (TiO_2) or zinc oxide (ZnO), is utilized, dye degradation can be efficient. The potential of the photocatalyst to yield reactive oxygen species (ROS) when exposed to light is essential. Solution pH: The pH of the solution can affect photocatalytic activity. Some photocatalysts respond more effectively at certain pH levels. TiO_2 , for example, is frequently more effective in slightly acidic or neutral environments. Electron Donors and Scavengers in the Solution: The presence of electron donors and scavengers in the solution might alter the degradation process. These species can compete with dye molecules or radicals for electrons, slowing down the process. Dye molecular structure: The chemical structure of the dye can impact its photocatalytic degradation susceptibility. Due to their chemical connections and functional groups, certain colors degrade more easily than others. The rate

of degradation of dye in the presence of the ZnAl_2O_4 sample was followed by the Pseudo-first order reaction kinetics (Elhalil et al., 2017):

$$\ln C_e = -kt + \ln C_0 \quad (4)$$

Where k (min^{-1}) is the rate constant and C_0 and C_e are the initial and equilibrium concentration of dye degradation at time t .

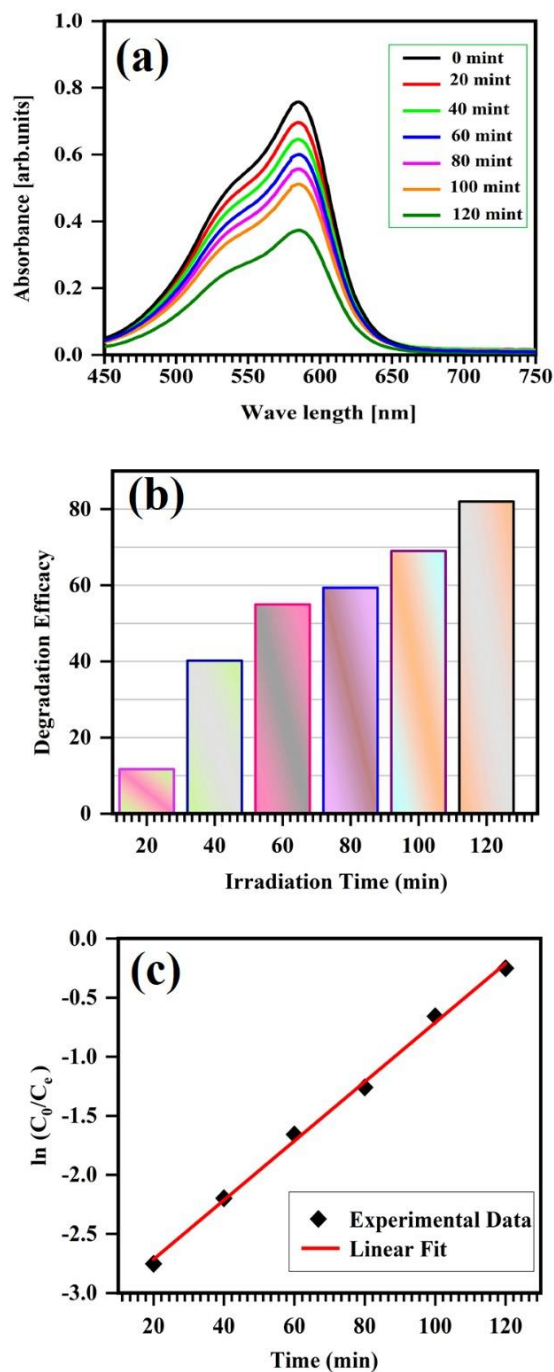


Figure 4. (a) Time-dependent degradation profile of crystal violet dye (b) Percent rate of degradation of crystal violet at different intervals of time (c) Pseudo-first order kinetic fit for degradation.

The value of the rate constant can be estimated from the slope of $\ln(C_0/C_e)$ vs irradiation time (t) as shown in Figure 4(c) and found to be 0.02505 per minute. The degradation rate constant of synthesized aluminate and other spinel-based photocatalysts used for the degradation of organic pollutants can vary depending on several factors, when exposed to light, aluminate spinels such as $MgAl_2O_4$, $CoAl_2O_4$, or $NiAl_2O_4$ are known for their photocatalytic activity in degrading organic contaminants. However, the actual degradation rate constant might vary greatly depending on the following factors:

Crystal Structure: The crystal structure of spinel-based materials can vary. The arrangement of atoms inside the crystal lattice can impact the degradation rate.

Synthesis route: The method utilized to synthesize the spinel-based photocatalyst can have a considerable influence on its characteristics. Different synthesis processes can result in materials with varying surface areas, particle sizes, and imperfections all of which can have an impact on photocatalytic activity.

Reaction Conditions: The photocatalytic activity of spinel-based photocatalysts can be influenced by factors such as pH, temperature, and the presence of other compounds.

Dye Concentration: Several variables can affect a catalyst's photocatalytic activity, including Dye Concentration: Generally, the rate of photocatalysis increases as the dye concentration increases. However, there may be an ideal concentration beyond which boosting the dye concentration does not improve the response rate considerably. This is because the active sites on the catalyst surface might get saturated at very high concentrations.

Catalyst type and Surface Area: The sort of catalyst utilized, as well as the surface area of the catalyst, can have a substantial impact on photocatalytic activity. $ZnAl_2O_4$ is a well-known photocatalyst whose characteristics, such as surface area and crystal structure, determine its performance. The photocatalytic activity of a catalyst can be affected by the presence of impurities in a solution. The extent of the impact depends on various factors, including the nature and concentration of the impurities, the properties of the catalyst, and the specific photocatalytic reaction under consideration.

The mechanism of crystal violet (CV) degradation under solar light irradiation is mentioned below

Solar Light Absorption: Crystal Violet molecules absorb visible light in the violet-blue part of the electromagnetic spectrum. This absorption causes electrons to be excited to higher energy states.

Electron Excitation: When photons are absorbed, electrons in the CV molecules become excited and migrate to higher energy levels. This stimulated state is not unstable.

Generation of Reactive Species: When Crystal Violet molecules are stimulated (CV^*), they can undergo a variety of photochemical reactions. One of the most prevalent mechanisms is the formation of reactive oxygen species (ROS) such as hydroxyl radicals ($\bullet OH$) and superoxide radicals ($\bullet O_2^-$) via energy or electron transfer.

Oxidation: The ROS produced are very reactive and can start the oxidation of Crystal Violet molecules. They can assault the CV molecules, leading the dye molecules to split into smaller fragments.

Mineralization: The degradation process might continue when the smaller fragments synthesized during the oxidation phase are further broken down into smaller and less complicated molecules.

Conclusion

Global population growth has increased the prevalence of environmental issues. Environmentally friendly photocatalysis and solar energy are required to substitute fossil fuels for the eradication of organic pollutants. In this contribution, we disclose the synthesis of ZnAl_2O_4 nanoparticles using the sol-gel auto-combustion method. The structural, morphologies, and optical properties of the prepared sample can be characterized by using XRD, FESEM, and UV-Vis spectroscopy. The photocatalytic performance of the synthesized catalyst was investigated for the degradation of Crystal violet dye. Significant removal of dye 80 % was achieved with a time irradiation of 120 min. The enhanced photocatalytic activity might be attributed to the citric acid molecule, in which four donor sites with metallic ions form chelating sites in which capping molecules provide superior stability to nanomaterials and a synergistic effect on their photocatalytic ability. ZnAl_2O_4 spinel, also known as zinc aluminate spinel, is a ceramic material with a wide range of industrial applications due to its excellent chemical, thermal, and mechanical properties which may potential applications in the field of wastewater treatment, refractories,

Acknowledgment

The authors are thankful to the Department of Physics, the University of Kotli for providing the laboratory facilities.

References

- Akpan, U., & Hameed, B. (2010). The advancements in sol-gel method of doped-TiO₂ photocatalysts. *Applied Catalysis A: General*, 375(1), 1–11.
- Anand, G. T., & Kennedy, L. J. (2013). One-Pot Microwave Combustion Synthesis of Porous $\text{Zn}_{1-x}\text{Cu}_x\text{Al}_2\text{O}_4$ ($0 \leq x \leq 0.5$) Spinel Nanostructures. *Journal of Nanoscience and Nanotechnology*, 13(4), 3096–3103.
- Anand, G. T., Kennedy, L. J., Aruldoss, U., & Vijaya, J. J. (2015). Structural, optical and magnetic properties of $\text{Zn}_{1-x}\text{Mn}_x\text{Al}_2\text{O}_4$ ($0 \leq x \leq 0.5$) spinel nanostructures by one-pot microwave combustion technique. *Journal of Molecular Structure*, 1084, 244–253.
- Ballarini, A. D., Bocanegra, S. A., Castro, A. A., De Miguel, S. R., & Scelza, O. A. (2009). Characterization of ZnAl_2O_4 obtained by different methods and used as catalytic support of Pt. *Catalysis Letters*, 129, 293–302.
- Bitla, Y., Chin, Y.-Y., Lin, J.-C., Van, C. N., Liu, R., Zhu, Y., Liu, H.-J., Zhan, Q., Lin, H.-J., & Chen, C.-T. (2015). Origin of metallic behavior in NiCo_2O_4 ferrimagnet. *Scientific Reports*, 5(1), 15201.
- Boppana, V. B. R., Doren, D. J., & Lobo, R. F. (2010). A Spinel Oxynitride with Visible-Light Photocatalytic Activity. *ChemSusChem*, 3(7), 814–817.

- Coulter, J. B., & Birnie III, D. P. (2018). Assessing Tauc plot slope quantification: ZnO thin films as a model system. *Physica Status Solidi (b)*, 255(3), 1700393.
- Elhalil, A., Elmoubarki, R., Machrouhi, A., Sadiq, M., Abdennouri, M., Qourzal, S., & Barka, N. (2017). Photocatalytic degradation of caffeine by ZnO-ZnAl₂O₄ nanoparticles derived from LDH structure. *Journal of Environmental Chemical Engineering*, 5(4), 3719–3726.
- El-Shobaky, H., Ghozza, A., El-Shobaky, G., & Mohamed, G. (1999). Physicochemical surface and catalytic properties of Cr₂O₃/Al₂O₃ system. *Colloids and Surfaces A: Physicochemical and Engineering Aspects*, 152(3), 315–326.
- Fakeeha, A. H., Al-Fatesh, A. S., Chowdhury, B., Ibrahim, A. A., Khan, W. U., Hassan, S., Sasudeen, K., & Abasaeed, A. E. (2018). Bi-metallic catalysts of mesoporous Al₂O₃ supported on Fe, Ni and Mn for methane decomposition: Effect of activation temperature. *Chinese Journal of Chemical Engineering*, 26(9), 1904–1911.
- Galetti, A. E., Gomez, M. F., Arrúa, L. A., & Abello, M. C. (2010). Ni catalysts supported on modified ZnAl₂O₄ for ethanol steam reforming. *Applied Catalysis A: General*, 380(1–2), 40–47.
- Grzybowska, B., Słoczyński, J., Grabowski, R., Weisło, K., Kozłowska, A., Stoch, J., cols, & Zieliński, J. (1998). Chromium oxide/alumina catalysts in oxidative dehydrogenation of isobutane. *Journal of Catalysis*, 178(2), 687–700.
- Ianoş, R., Boreănescu, S., & Lazău, R. (2014). Large surface area ZnAl₂O₄ powders prepared by a modified combustion technique. *Chemical Engineering Journal*, 240, 260–263.
- Kirankumar, V., & Sumathi, S. (2020). A review on photodegradation of organic pollutants using spinel oxide. *Materials Today Chemistry*, 18, 100355.
- Lee, K. M., Lai, C. W., Ngai, K. S., & Juan, J. C. (2016). Recent developments of zinc oxide based photocatalyst in water treatment technology: A review. *Water Research*, 88, 428–448.
- Lv, W., Liu, B., Qiu, Q., Wang, F., Luo, Z., Zhang, P., & Wei, S. (2009). Synthesis, characterization and photocatalytic properties of spinel CuAl₂O₄ nanoparticles by a sonochemical method. *Journal of Alloys and Compounds*, 479(1–2), 480–483.
- Manikandan, A., Vijaya, J. J., Mary, J. A., Kennedy, L. J., & Dinesh, A. (2014). Structural, optical and magnetic properties of Fe₃O₄ nanoparticles prepared by a facile microwave combustion method. *Journal of Industrial and Engineering Chemistry*, 20(4), 2077–2085.
- Mote, V., Purushotham, Y., & Dole, B. (2012). Williamson-Hall analysis in estimation of lattice strain in nanometer-sized ZnO particles. *Journal of Theoretical and Applied Physics*, 6, 1–8.
- Motloug, S., Dejene, F., Swart, H., & Ntwaeaborwa, O. (2015). Effects of Zn/citric acid mole fraction on the structure and luminescence properties of the un-doped and 1.5% Pb²⁺ doped ZnAl₂O₄ powders synthesized by citrate sol–gel method. *Journal of Luminescence*, 163, 8–16.
- Petcharoen, K., & Sirivat, A. (2012). Synthesis and characterization of magnetite nanoparticles via the chemical co-precipitation method. *Materials Science and Engineering: B*, 177(5), 421–427.
- Robinson, L. N. (2008). *Water resources research progress*. Nova Publishers.

- Selvanayagi, R., Rameshbabu, M., Muthupandi, S., Razia, M., Florence, S. S., Ravichandran, K., & Prabha, K. (2022). Structural, optical and electrical conductivity studies of pure and Fe doped ZincOxide (ZnO) nanoparticles. *Materials Today: Proceedings*, 49, 2628–2631.
- Sickafus, K. E., Wills, J. M., & Grimes, N. W. (1999). Structure of spinel. *Journal of the American Ceramic Society*, 82(12), 3279–3292.
- Srinatha, N., Kumar, K. R., Kumar, M. S., Madhu, A., & Angadi, B. (2022). A novel combustion fuel for the synthesis of nanocrystalline ZnAl₂O₄ particles based on the thermodynamic correlations and their structural and optical studies. *Ceramics International*, 48(3), 3669–3675.
- Sunder, S., & Kumar, A. (n.d.). Study of ZnAl₂O₄ Prepared by Co-precipitation Method. *Shyam Sunder*, 1, 54–56.
- Sutka, A., & Meziniskis, G. (2012). Sol-gel auto-combustion synthesis of spinel-type ferrite nanomaterials. *Frontiers of Materials Science*, 6, 128–141.
- Tang, J., Zou, Z., & Ye, J. (2004). Efficient photocatalytic decomposition of organic contaminants over CaBi₂O₄ under visible-light irradiation. *Angewandte Chemie*, 116(34), 4563–4566.
- Tao, J., Jiang, W., Pan, H., Xu, X., & Tang, R. (2007). Preparation of large-sized hydroxyapatite single crystals using homogeneous releasing controls. *Journal of Crystal Growth*, 308(1), 151–158.
- Tian, X., Wan, L., Pan, K., Tian, C., Fu, H., & Shi, K. (2009). Facile synthesis of mesoporous ZnAl₂O₄ thin films through the evaporation-induced self-assembly method. *Journal of Alloys and Compounds*, 488(1), 320–324.
- Védrine, J. C. (2017). Heterogeneous catalysis on metal oxides. *Catalysts*, 7(11), 341.
- Wang, D., Zou, Z., & Ye, J. (2003). A new spinel-type photocatalyst BaCr₂O₄ for H₂ evolution under UV and visible light irradiation. *Chemical Physics Letters*, 373(1–2), 191–196.
- Wang, S.-F., Sun, G.-Z., Fang, L.-M., Lei, L., Xiang, X., & Zu, X.-T. (2015). A comparative study of ZnAl₂O₄ nanoparticles synthesized from different aluminum salts for use as fluorescence materials. *Scientific Reports*, 5(1), 12849.
- Weckhuysen, B. M., & Schoonheydt, R. A. (1999). Olefin polymerization over supported chromium oxide catalysts. *Catalysis Today*, 51(2), 215–221.
- Zhang, W., Wang, Y., Shen, Y., Xie, M., & Guo, X. (2016). Mesoporous zinc aluminate (ZnAl₂O₄) nanocrystal: Synthesis, structural characterization and catalytic performance towards phenol hydroxylation. *Microporous and Mesoporous Materials*, 226, 278–283.
- Zhu, Z., Li, X., Zhao, Q., Li, H., Shen, Y., & Chen, G. (2010). Porous “brick-like” NiFe₂O₄ nanocrystals loaded with Ag species towards effective degradation of toluene. *Chemical Engineering Journal*, 165(1), 64–70.